Published online 19 August 2009

Nucleic Acids Research, 2009, Vol. 37, No. 18 ***6259–6268***
doi:10.1093/nar/gkp648

Crystal structure of human selenocysteine tRNA

Yuzuru Itoh[1,2], Shiho Chiba[1], Shun-ichi Sekine[1,2] and Shigeyuki Yokoyama[1,2,*]

[1]Department of Biophysics and Biochemistry, Graduate School of Science, The University of Tokyo, 7-3-1 Hongo, Bunkyo-ku, Tokyo 113-0033 and [2]RIKEN Systems and Structural Biology Center, 1-7-22 Suehiro-cho, Tsurumi, Yokohama 230-0045, Japan

Received June 23, 2009; Revised July 18, 2009; Accepted July 20, 2009

ABSTRACT

Selenocysteine (Sec) is the 21st amino acid in translation. Sec tRNA ($tRNA^{Sec}$) has an anticodon complementary to the UGA codon. We solved the crystal structure of human $tRNA^{Sec}$. $tRNA^{Sec}$ has a 9-bp acceptor stem and a 4-bp T stem, in contrast with the 7-bp acceptor stem and the 5-bp T stem in the canonical tRNAs. The acceptor stem is kinked between the U6:U67 and G7:C66 base pairs, leading to a bent acceptor-T stem helix. $tRNA^{Sec}$ has a 6-bp D stem and a 4-nt D loop. The long D stem includes unique A14:U21 and G15:C20a pairs. The D-loop:T-loop interactions include the base pairs G18:U55 and U16:U59, and a unique base triple, U20:G19:C56. The extra arm comprises of a 6-bp stem and a 4-nt loop. Remarkably, the D stem and the extra arm do not form tertiary interactions in $tRNA^{Sec}$. Instead, $tRNA^{Sec}$ has an open cavity, in place of the tertiary core of a canonical tRNA. The linker residues, A8 and U9, connecting the acceptor and D stems, are not involved in tertiary base pairing. Instead, U9 is stacked on the first base pair of the extra arm. These features might allow $tRNA^{Sec}$ to be the target of the Sec synthesis/incorporation machineries.

INTRODUCTION

Selenocysteine (Sec) is known as the 21st amino acid used in translation (1,2). Its structure is similar to that of cysteine (Cys), and the selenium atom in Sec corresponds to the sulfur atom in Cys. The selenol group in Sec is more nucleophilic than the thiol group in Cys, with pK_a values of ~5.2 and ~8.5, respectively (3). Therefore, the Sec residue is primarily used at the active center for oxidation-reduction reactions (4–6). Sec and its biosynthesis/insertion machineries are widely distributed from bacteria to humans, and are essential for their viability. Humans have 25 selenoproteins (7).

In contrast to the other amino acids, Sec is synthesized on the Sec-specific tRNA species ($tRNA^{Sec}$) through a multistep process. $tRNA^{Sec}$ is first aminoacylated with serine by seryl-tRNA synthetase (SerRS) (8). In eukarya and archaea, the hydroxyl group of the seryl moiety is further phosphorylated by *O*-phosphoseryl-tRNA kinase (PSTK) (9). The phosphate group is then converted to the selenol group by Sep-tRNA:Sec-tRNA synthase (SepSecS), to produce selenocysteinyl-$tRNA^{Sec}$ (Sec-$tRNA^{Sec}$) (10,11). In bacteria, Ser-$tRNA^{Sec}$ is directly converted to Sec-$tRNA^{Sec}$ by Sec synthase (SecS or SelA) (12). The selenophosphate generated by selenophosphate synthetase (SPS) is utilized as a reactive selenium donor for Sec synthesis in both eukarya/archaea and bacteria (13,14).

$tRNA^{Sec}$ has the anticodon complementary to the stop codon UGA (8), and translates it in a selenoprotein messenger RNA (mRNA) to Sec, in response to a Sec-insertion sequence (SECIS) (15,16). Sec-specific translation elongation factor (EF-Sec, SelB) brings Sec-$tRNA^{Sec}$ to the ribosome in response to the SECIS (17–20), and Sec is then incorporated into a nascent, growing polypeptide, by decoding the UGA codon. Thus, $tRNA^{Sec}$ plays a vital role in both the Sec biosynthesis and its insertion into selenoproteins. Bacterial SelB directly recognizes SECIS (18,21,22), while eukaryal/archaeal EF-Sec needs an additional factor for SECIS recognition (23,24). SECIS binding protein 2 (SBP2) recognizes SECIS in eukarya (23,25), but the additional factor has not been identified yet in archaea. Another factor, SECp43, is involved in the Sec synthesis and insertion in eukarya (26,27), but the precise function of SECp43 is not known.

$tRNA^{Sec}$ is the largest among known tRNA species; it consists of 90–100-nt residues, in contrast to most other tRNAs, with ~76-nt residues (28) (Figure 1A–C). Biochemical analyses using enzymatic and chemical probes revealed the unique structure of $tRNA^{Sec}$ (29,30). It has a long extra arm, similar to those of the serine, leucine and tyrosine tRNAs. However, eukaryal/archaeal $tRNA^{Sec}$ has a 9-bp acceptor stem and a 4-bp T stem

*To whom correspondence should be addressed. Tel: +81 3 5841 4392; Fax: +81 3 5841 8057; Email: yokoyama@biochem.s.u-tokyo.ac.jp

The authors wish it to be known that, in their opinion, the first two authors should be regarded as joint First Authors.

(9/4 secondary structure), and bacterial $tRNA^{Sec}$ has an 8-bp acceptor stem and a 5-bp T stem (8/5 secondary structure). In both the eukaryal/archaeal and bacterial $tRNA^{Sec}$s, the acceptor and T stems have 13 bp in total. Conversely, the canonical tRNAs have a 7-bp acceptor stem and a 5-bp T stem (7/5 secondary structure) (Figure 1A–C). $tRNA^{Sec}$ also has a 6-bp D-stem and a 4-nt D-loop, in contrast to the 4-bp D-stem and approximately 8-nt D-loop in the canonical tRNAs. The unique structure presumably allows $tRNA^{Sec}$, like $tRNA^{Ser}$, to function as a substrate of SerRS, and, in contrast, as the exclusive target of PSTK, SepSecS (or SelA), and EF-Sec. Despite its significance and distinctive features, the 3D structure of $tRNA^{Sec}$ has not yet been solved.

Here, we report the crystal structure of human $tRNA^{Sec}$. The structure revealed the unusual secondary structures of the acceptor, T and D stems, as well as unique tertiary interactions. In contrast with the usual tRNAs, the long D stem of $tRNA^{Sec}$ does not interact with the extra arm, and thus, $tRNA^{Sec}$ has an open cavity in place of the hydrophobic core.

MATERIALS AND METHODS

Preparation of human $tRNA^{Sec}$

To synthesize the template DNA for the transcription of human $tRNA^{Sec}$, the following oligonucleotides were used: 5′-GGTGGTggatcc**TAATACGACTCACTATA**GC CCGGATGATCCTCAGTGGTCTGGGGTGCAGGC TTCAAACCT-3′ and 5′-GGTGGTgcatgcCCTGGCGCC CGAAAGGTGGAATTGAACCACTCTGTCGCTAG ACAGCTACAGGTTTGAAGCCT-3′. The underlined 3′ regions are complementary to each other for annealing. After annealing, the 3′-ends were both extended by overlap extension polymerase chain reaction (OE-PCR). The synthesized DNA includes the consensus sequence of T7 RNA polymerase promoters, just upstream of the $tRNA^{Sec}$ gene (indicated as bold letters). BamHI and SphI sites were placed at the upstream and downstream ends, respectively, for cloning. The synthesized fragment was cloned between the BamHI and SphI sites of the pUC18 vector (Roche).

Using this plasmid as a template, the DNA region containing the $tRNA^{Sec}$ gene was amplified by PCR and used as the template for *in vitro* transcription. The M13-reverse primer and a primer complementary to the 3′ end of the target tRNA (5′-TGGCGCCCGAAAGGTG GAATTG-3′) were used for PCR.

Human $tRNA^{Sec}$ was transcribed *in vitro* with T7 RNA polymerase, as described previously (31). The transcribed $tRNA^{Sec}$ was purified by anion-exchange chromatography using a ResourceQ (GE-Healthcare Bio-Sciences) column. The $tRNA^{Sec}$ was dissolved in 10 mM Tris–HCl buffer (pH 8.0) containing 10 mM $MgCl_2$, and was heated at 65°C for 5 min for refolding.

Preparation of *Methanocaldococcus jannaschii* SepSecS

Methanocaldococcus jannaschii SepSecS gene was cloned into pET22b (Merck). The protein was overexpressed in *Escherichia coli* Rosetta 2(DE3) (Merck) transformed by the vector. The cells were sonicated, heat-treated at 85°C and purified by successive chromatography steps on a Phenyl-Toyopearl (Tosoh) column with a gradient of 1.8–0.0 M ammonium sulfate, and a SP-Sepharose FF (GE-Healthcare) column with a gradient of 0.05–0.6 M NaCl. SepSecS-containing fractions were pooled and dialyzed against 20 mM Tris–HCl buffer (pH 7.5), containing 300 mM NaCl and 10 mM 2-mercaptoethanol (2-ME).

Crystallization and X-ray diffraction data collection

$tRNA^{Sec}$ was dissolved in 20 mM Tris–HCl buffer (pH 7.5), containing 300 mM NaCl, 10 mM $MgCl_2$ and 10 mM 2-ME, and the concentration was adjusted to 120 μM. This sample solution also contained 80 μM *M. jannaschii* SepSecS. The mixture was heated at 65°C for 10 min and gradually cooled to room temperature. Crystal Screen 2, Natrix (Hampton Research), and Wizard I and II (Emerald BioSystems) kits were used for the initial screening of crystallization conditions. Crystals were obtained with Crystal Screen 2 Reagent 13, and the conditions were further optimized. Crystals suitable for data collection were obtained by mixing 0.75-μl sample solution and 0.75-μl reservoir solution, containing 100 mM sodium acetate-HCl buffer (pH 4.1), 32% (w/v) polyethylene glycol (PEG) 1500 and 140 mM lithium sulfate, and by equilibrating the mixture against 200-μl reservoir solution at 20°C by the sitting-drop vapor-diffusion method. We confirmed that the crystals contained only $tRNA^{Sec}$ by SDS–PAGE and urea–PAGE analyses (data not shown). No crystal was obtained when sample solutions without SepSecS were used.

Prior to data collection, the crystals were soaked in a cryo-protective solution, containing 100 mM sodium acetate–HCl (pH 4.6), 35% (w/v) PEG 1000, 25 mM ammonium sulfate and 10 mM $MgCl_2$, and were flash-cooled with liquid nitrogen. A 3.1-Å X-ray diffraction data set was obtained by using the synchrotron radiation at BL41XU of SPring-8 (Hyogo, Japan). The data were indexed, integrated and scaled with the HKL2000 program (32) (Table 1). The crystals belong to the space group $C2$, with unit cell parameters $a = 78.9$, $b = 51.6$, $c = 81.4$ Å, $\beta = 101.6°$.

Structure determination and refinement

The human $tRNA^{Sec}$ crystal structure was solved by the molecular replacement method with the Phaser program (33). Partial structures from the $tRNA^{Asp}$ and $tRNA^{Phe}$ coordinates [PDB ID: 2TRA (34) and 6TNA (35)] were used as the search models. The nucleotide sequences of the $tRNA^{Asp}$ and $tRNA^{Phe}$ structures were replaced by that of human $tRNA^{Sec}$. The search model used for the first round of molecular replacement was composed of the acceptor stem (residues 1–7 and 66–72), the T arm (residues 49–65) and part of the D loop (residues 18 and 19) of the sequence-modified $tRNA^{Asp}$. The search solution (solution I) was obtained just for the corresponding part of the $tRNA^{Sec}$. Solution I was refined against the

diffraction data by positional energy minimization refinement with the CNS program (36). The second round was done using the refined solution I as a fixed model. The search model used for the second round was the anticodon-arm part (residues 26–44) of the sequence-modified $tRNA^{Phe}$ structure. The second search solution (solution II) identified the extra-arm stem of the human $tRNA^{Sec}$. Solution II was also refined and used as the fixed model for the final round. The search model used for the final round was the anticodon stem (residues 26–31 and 39–44) of the sequence-modified $tRNA^{Asp}$ structure. The final search solution yielded the anticodon stem of the $tRNA^{Sec}$. The D-arm portion of $tRNA^{Sec}$ was not found by the molecular replacement, and its coordinates were built in an $|F_o\text{-}F_c|$ electron density map.

The structure was refined against the diffraction data by iterative cycles of simulated-annealing, positional and temperature-factor refinements with the CNS program (36), and manual model building and revision with the Coot program (37). Multiple rounds of refinement generated the convergence of the R_{work} and R_{free} to 0.254 and 0.314, respectively (Table 1). The R_{work} and R_{free} are relatively higher than those of the reported crystal structures of RNAs, possibly due to the missing tRNA terminus and the partially disordered anticodon loop.

Docking model construction

The docking model of SerRS and $tRNA^{Sec}$ was created based on the structure of the *Thermus thermophilus* SerRS•$tRNA^{Ser}$ complex [PDB ID: 1SER (38)]. We used the structure of SerRS from the archaeon *Pyrococcus horikoshii* [PDB ID: 2DQ0 (39)], as a model of a eukaryal SerRS. SerRS in *T. thermophilus* SerRS•$tRNA^{Ser}$ was replaced by *P. horikoshii* SerRS, as described previously (39). The *T. thermophilus* $tRNA^{Ser}$ structure was then replaced by human $tRNA^{Sec}$. The extra stem and the T arm were used for the superposition (residues 45–47c, 47h–48 and 50–64 in $tRNA^{Sec}$ versus residues 45–47c, 47l–47q and 50–64 in $tRNA^{Ser}$).

The present $tRNA^{Sec}$ structure was docked onto the complex structure of *Thermus aquaticus* EF-Tu and *Saccharomyces cerevisiae* $tRNA^{Phe}$ [PDB ID: 1TTT (40)]. $tRNA^{Phe}$ in the EF-Tu•$tRNA^{Phe}$ complex was replaced by human $tRNA^{Sec}$, to create the EF-Tu•$tRNA^{Sec}$ docking model. The 12 bp of the acceptor-T stem of human $tRNA^{Sec}$ (residues 1–7, 50–52 and 62–72) and those of $tRNA^{Phe}$ (residues 1–7, 49–53 and 61–72) were used as the corresponding region for the superposition. Furthermore, EF-Tu in the EF-Tu•$tRNA^{Sec}$ docking model was replaced by *Methanococcus maripaludis* SelB/EF-Sec [PDB ID: 1WB3 (41)], to create the EF-Sec•$tRNA^{Sec}$ docking model. Homologous domains I–III were used for the superposition.

RESULTS

Structure determination

Human $tRNA^{Sec}$ was prepared by *in vitro* transcription with T7 RNA polymerase. Single crystals of $tRNA^{Sec}$ were obtained under conditions containing *M. jannaschii* SepSecS. The crystal structure was solved by molecular replacement, using the RNA helix or hairpin portions of reported tRNA structures [$tRNA^{Asp}$ (34) and $tRNA^{Phe}$ (35)] as the search models. The resolution is 3.1 Å and the final refinement *R* factors, R_{work} and R_{free}, are 0.254 and 0.314, respectively (Table 1). The crystals contained one $tRNA^{Sec}$ molecule per asymmetric unit. Human $tRNA^{Sec}$ is composed of 90-nt residues (numbered as residues 1–76 in the conventional manner), and the final model includes 86 residues (residues 1–72). The four 3′-end residues, the discriminator G73 and the CCA end (residues 74–76), were disordered.

Table 1. Data collection and refinement statistics

PDB ID	3A3A
Data collection	
Wave length (Å)	1.000
Space group	*C*2
Cell dimensions	$a = 78.9$, $b = 51.6$, $c = 81.4$ Å, $\beta = 101.6°$
Resolution (Å)	50.0–3.10 (3.21–3.10)
Unique reflections	5833
Completeness (%)	96.7 (85.9)
Redundancy	5.4 (5.4)
R_{sym}[a]	0.105 (0.390)
Mean $I/\sigma(I)$	18.0 (3.53)
Structure refinement	
Working set reflections	5523
Test set reflections	258
Resolution (Å)	50.0–3.10
No. of RNA residues	86
No. of RNA atoms	1829
R_{work}/R_{free}[b]	0.254/0.314
Average *B* factor (Å^2)	115.0
RMSD values of bond lengths (Å)	0.0046
RMSD values of bond angles (°)	0.92

[a] $R_{sym} = \sum_{hkl}\sum_i[|I_i(hkl) - <I(hkl)>|]/\sum_{hkl}\sum_i[I_i(hkl)]$, where $I_i(hkl)$ is the intensity of the *i*-th measurement of *hkl* and $<I(hkl)>$ is the average value of $I_i(hkl)$ for all *i* measurements.
[b] $R_{work} = \sum_{hkl}(||F_{obs}| - k|F_{calc}||)/\sum_{hkl}(|F_{obs}|)$, $R_{free} = \sum_{hkl\text{Test}}(||F_{obs}| - k|F_{calc}||)/\sum_{hkl\text{Test}}(|F_{obs}|)$, where *hkl*Test is the test set reflections that were not used during refinement (4.5% of the data set).

The $tRNA^{Sec}$ structure revealed that it consists of the 9-bp acceptor stem (residues 1–5, 5a, 5b, 6, 7, 66, 67, 67a, 67b and 68–72), the linker between the acceptor stem and the D stem ('AD linker', residues 8 and 9), the D arm (a 6-bp stem and a 4-nt loop, residues 10–16, 18–20, 20a and 21–25), the anticodon arm (a 6-bp stem and a 7-nt loop, residues 26–44), the extra arm (a 6-bp stem and a 4-nt loop, residues 45–47, 47a–47l and 48) and the T arm (a 4-bp stem and a 7-nt loop, residues 50–64) (Figure 1A, D and G). The nucleotide numbering is based on Sturchler *et al.* (29)

Several modified nucleosides have been reported in vertebrate $tRNA^{Sec}$s, such as 5-methylcarboxymethyluridine (mcm^5U) or O2′-methylated mcm^5U (mcm^5Um) at position 34, N^6-isopentyladenosine (i^6A) at position 37, pseudouridine (Ψ) at position 55 and 1-methyladenosine (m^1A) at position 58 (42,43). The human $tRNA^{Sec}$ used for crystallization was synthesized by *in vitro* transcription, and thus lacks modified nucleosides.

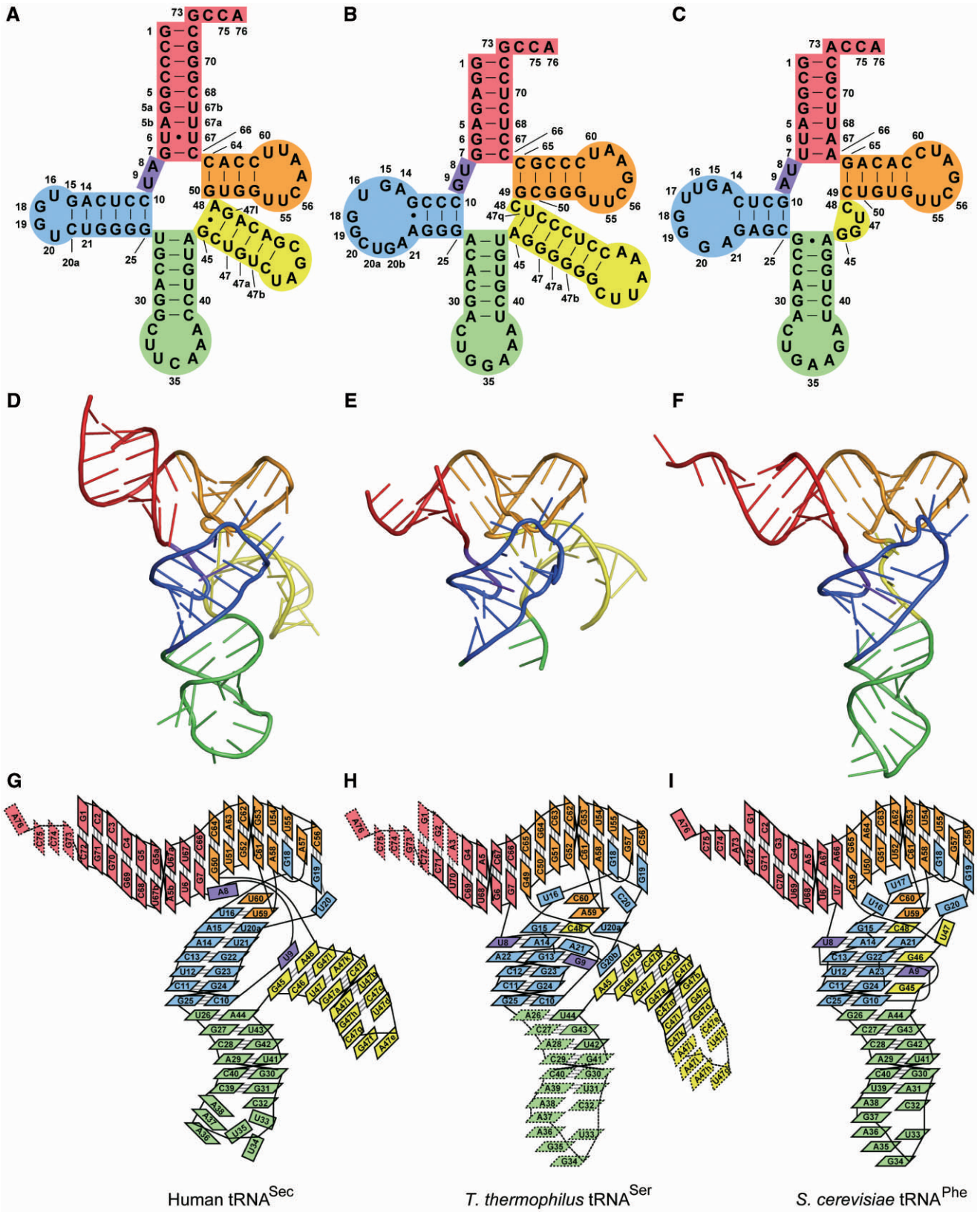

Figure 1. Structure of human $tRNA^{Sec}$, and its comparison with other tRNAs. Human $tRNA^{Sec}$ is shown as a cloverleaf model (**A**), a ribbon model (**D**) and a diagram representing tertiary interactions (**G**). For comparison, *T. thermophilus* $tRNA^{Ser}$ [PDB ID: 1SER (38)] (**B**, **E** and **H**) and *S. cerevisiae* $tRNA^{Phe}$ [PDB ID: 4TNA (47)] (**C**, **F** and **I**) are shown. The acceptor arm, AD linker, D arm, anticodon arm, extra arm and T arm are colored red, purple, blue, green, yellow and orange, respectively.

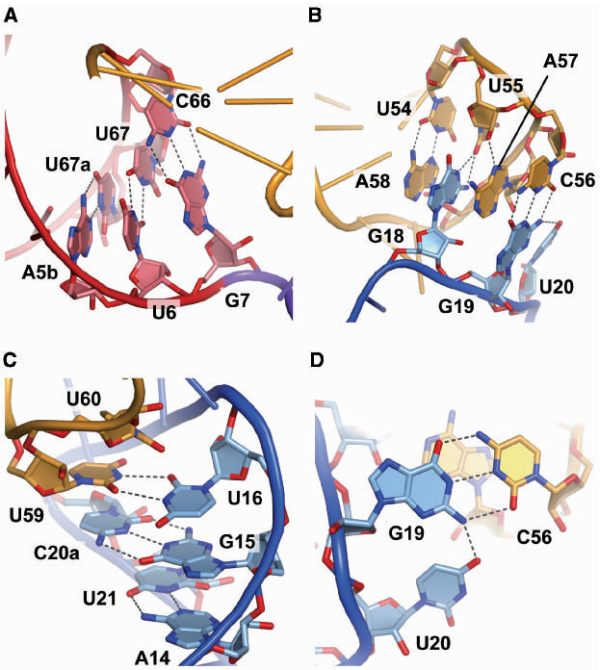

Figure 2. tRNA^{Sec}-specific base pairs and base triples. (**A**) The U6:U67 base pair in the acceptor stem. (**B**) The interface of the D and T loops at the tRNA elbow. (**C**) The A14:U21, G15:C20a and U16:U59 base pairs in the D arm. (**D**) The U20:G19:C56 base triple. The structural models are colored as in Figure 1.

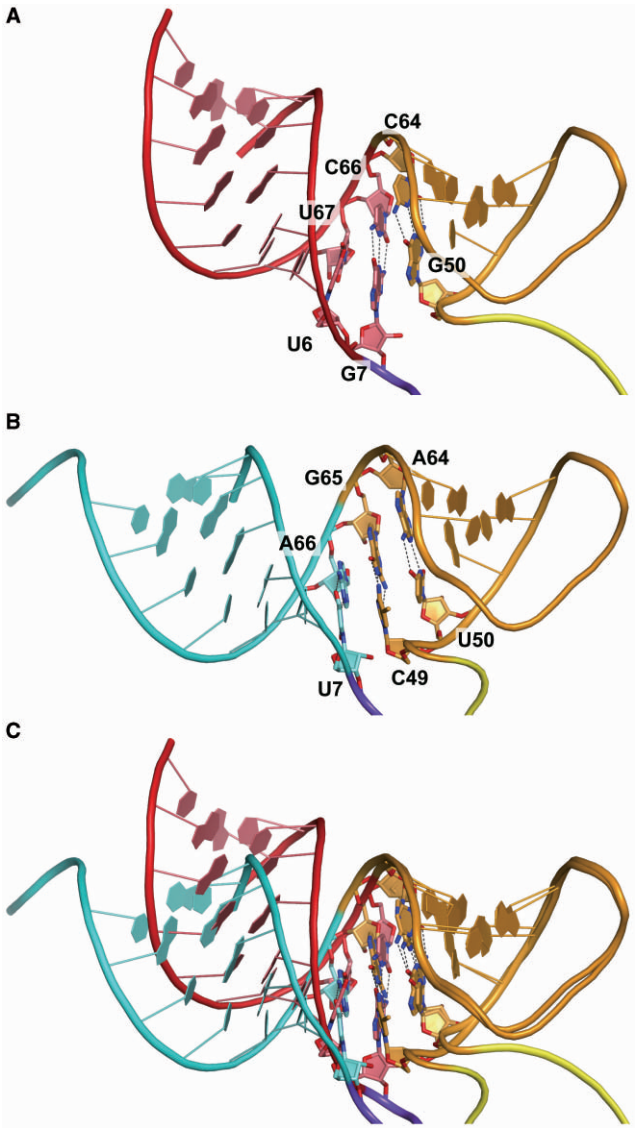

Figure 3. The bent acceptor-T stem helix. (**A**) The acceptor and T arms of human tRNA^{Sec}, colored as in Figure 1. (**B**) The acceptor and T arms of *S. cerevisiae* tRNA^{Phe} for comparison. The acceptor arm of *S. cerevisiae* tRNA^{Phe} is colored cyan. (**C**) The acceptor and T arms of tRNA^{Sec} are superposed on those of tRNA^{Phe}. The phosphate atoms of the T arm residues (residues 50–64) were used as the corresponding atoms for the superposition.

The acceptor and T arms

tRNA^{Sec} has a 9-bp acceptor stem and a 4-bp T stem (9/4 secondary structure), in contrast to the canonical tRNAs (7/5 secondary structure) (Figure 1). The T loop is composed of seven residues, and its conformation is similar to those of the canonical tRNAs (38,44–47). U54 forms a reversed Hoogsteen base pair with A58. As in the canonical tRNAs, U55 and C56 form tertiary interactions with G18 and G19, respectively, in the D loop (Figure 2B). Therefore, the lack of the Ψ55 and m^{1}A58 modifications does not appear to affect the tertiary structure due the T-loop:D-loop interaction.

U6 and U67 in the acceptor stem are highly conserved among the eukaryal tRNA^{Sec}s (Supplementary Figure 1), and they form a non-Watson–Crick-type (non-WC-type) base pair (Figure 2A). The acceptor stem is kinked between the U6:U67 and G7:C66 base pairs, resulting in a bent acceptor-T helix (Figure 3A and C). This is in contrast with the continuous acceptor-T helix observed in many tRNA structures (44–47) (Figure 3B and C). The G1:C72 base pair shares a crystal contact with the G19:C56 base pair in the other molecule in the crystal. We speculate that the acceptor-T helix is bent due to the crystal contact, and therefore is probably straight in solution. Nevertheless, the bent acceptor-T helix may mimic a conformational state required for interactions with other factors, e.g. EF-Sec, as discussed below.

The D arm and tertiary interactions

The D arm (residues 10–16, 18–20, 20a and 21–25) is the hairpin structure composed of a 6-bp stem (D stem) and a 4-nt loop (D loop). The D loop of tRNA^{Sec} comprises only 4-nt residues, U16, G18, G19 and U20, in contrast to those of the canonical tRNAs (7–11 residues). In spite of the small D loop, the D-loop:T-loop interactions (the G18:U55 and G19:C56 base pairs) are conserved (Figure 2B). U16 forms a non-WC-type interaction with U59 (Figure 2C), while other types of the 16:59 pair are also found in a few canonical tRNAs (40,48). The U16:U59 pair is sandwiched between the sixth base pair of the D stem (the G15:C20a pair) and U60 in the T loop (Figure 2C). The last D-loop residue, U20, interacts with G19 to form a base triple (U20:G19:C56) (Figure 2B and D).

The D stem has 6 bp, as it includes the A14:U21 and G15:C20a pairs, which are found only in tRNA^{Sec} (Figure 2C). Remarkably, none of the D-stem residues participates in tertiary interactions. The tertiary interactions are limited to those between the D and T loops. This is in a sharp contrast with the fact that the D stem interacts with the AD linker (residues 8 and 9) and the extra arm (residues 45–48) to form a core of tertiary interactions in the canonical tRNAs. These include the conserved pairs U8:A14 and R15:Y48, where R and Y denote G/A and C/U, respectively, and some non-conserved pairs, 9:23, 9:13, 10:45 and 22:46 (38,44,45). Probably due to the lack of these interactions, the D stem of tRNA^{Sec} is shifted outward from the axis running along the anticodon stem to the T loop (Figure 4A). In other words, tRNA^{Sec} has an open cavity instead of the conventional tertiary core.

The AD linker in tRNA^{Sec} (A8 and U9) occupies a completely different position from those of the canonical tRNAs. A8 is not involved in tertiary base pairs. Instead, the adenine ring is surrounded by A48 and G50, and the O2′ atom hydrogen bonds with that of A48 (Figure 4C). In the canonical tRNAs, the conserved U8 has a reversed Hoogsteen interaction with A14 in the D arm (the U8:A14 pair) (38,44,45). U9 in tRNA^{Sec} is stacked on the first base pair of the extra-arm stem ('extra stem') (Figure 4E). In the canonical tRNAs, the residue at position 9 interacts with a D-stem residue to form a base triple, such as the 12:23:9 or 9:13:22 pair (38,44,45).

The anticodon arm

The structure of the tRNA^{Sec} anticodon arm (residues 26–44) is similar to those of the canonical tRNAs. Although the anticodon loop has an irregular conformation (Figure 1D), this is probably due to the crystal contact and/or lack of modification, and may not reflect the unique features of tRNA^{Sec}. Several nucleotide modifications have been reported for eukaryal tRNA^{Sec}, and some of them are located in the anticodon loop, e.g. mcm^{5}U or mcm^{5}Um at position 34, and i^{6}A at position 37 (42,43). These modified nucleotides may reinforce the anticodon loop conformation, and contribute toward stabilizing the codon:anticodon pairing on the ribosome.

The extra arm

The extra arm (residues 45–47, 47a–47l and 48) forms a hairpin structure composed of a 6-bp stem and a 4-nt loop. G45 and A48 form a non-WC G45:A48 base pair, which is the first base pair of the extra stem (Figure 4E). None of the residues in the extra arm is involved in tertiary base pairing with the other arms. In the canonical tRNAs, Y48 interacts with R15 in the D arm, to form the Levitt pair (38,44,45). In the reported structure of tRNA^{Ser} from the bacterium *T. thermophilus*, the linker between the extra stem and the T stem is C48 (Figure 1B and H). C48 is base paired with G15, and is connected to G49 in the T stem (Figure 4D and F) (38). tRNA^{Sec} lacks such a linker residue, as A48 base pairs with G45, and the G45:A48 pair occupies the position corresponding to the A45:U47q pair in *T. thermophilus* tRNA^{Ser} (Figures 1A and B; 4E and F). A48 is directly connected to G50, thus shortcutting the Levitt pair and the 49:65 pair (Figure 4C and E).

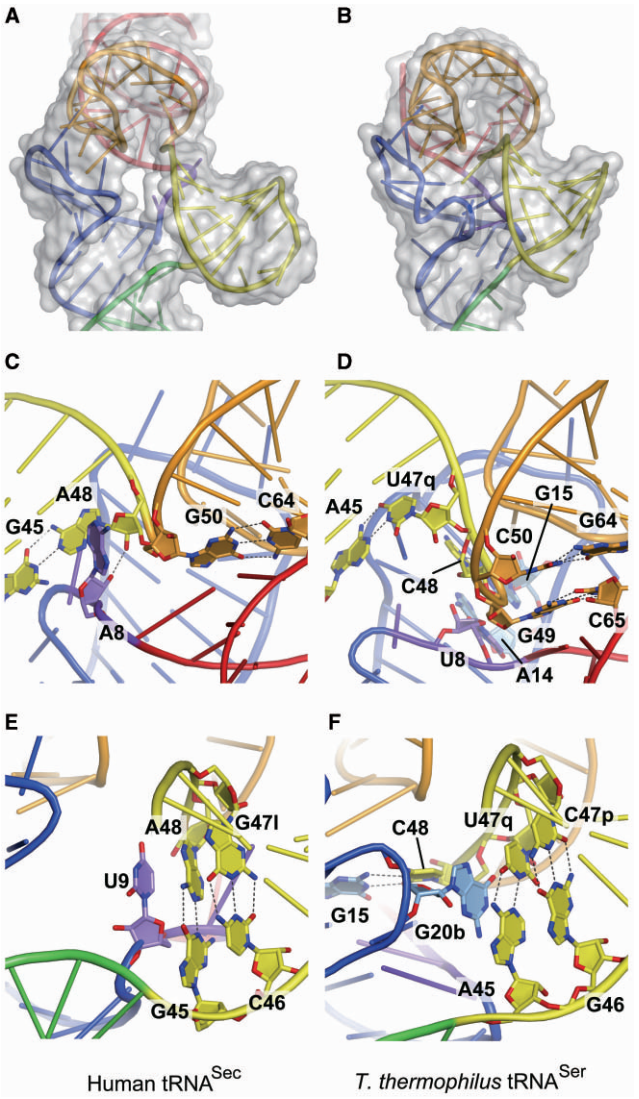

Figure 4. Unique features in tRNA^{Sec}. (**A** and **B**) The D, T and extra arms of human tRNA^{Sec} (A) and *T. thermophilus* tRNA^{Ser} (B) are shown with their surface models. There is an open cavity in tRNA^{Sec}. (**C** and **E**) Close-up views showing the interactions between the AD linker residues and the first base pair of the extra stem. (**D** and **F**) The corresponding regions in *T. thermophilus* tRNA^{Ser} are shown for comparison. (C) A8 in human tRNA^{Sec}. (D) U8 in *T. thermophilus* tRNA^{Ser}. (E) U9 and the first extra-stem base pair (G45:A48) in human tRNA^{Sec}. (F) G20b and the first extra-stem base pair in *T. thermophilus* tRNA^{Ser}.

In human tRNA^{Sec}, U9 is stacked on the first base pair of the extra stem (the G45:A48 pair) (Figure 4E). In *T. thermophilus* tRNA^{Ser}, G20b in the D loop occupies the corresponding position (Figure 4F) (38). Although the secondary structures and tertiary interactions are different between human tRNA^{Sec} and *T. thermophilus* tRNA^{Ser}, the orientations of their extra stems against their T arms are nearly identical (Figure 4A and B). This partially explains the fact that both tRNA^{Ser} and

tRNA^{Sec} are aminoacylated with serine by the same enzyme, SerRS.

DISCUSSION

The tRNA^{Sec} structure

We solved the crystal structure of human tRNA^{Sec}. The structure revealed that the acceptor stem of a eukaryal tRNA^{Sec} has 9 bp, and the T stem has 4 bp (the 9/4 secondary structure). Conversely, bacterial tRNA^{Sec}s have the 8/5 secondary structure and the canonical tRNAs have the 7/5 secondary structure (28). In the present structure, the acceptor-T stem is bent between the U6:U67 and G7:C66 base pairs (Figure 3A and C), although it is unclear whether this bending reflects a physiological tRNA^{Sec} conformation. The D arm is composed of a 6-bp stem and a 4-nt loop. The interaction between the D and T loops is normal, but the D arm lacks tertiary interaction with the AD linker and the extra arm. As revealed by the hole between the D and extra arms, the tertiary interactions in tRNA^{Sec} are less complicated than those in the canonical tRNAs (Figure 4A). This unique global feature of the tertiary structure with respect to the unusually long D stem of tRNA^{Sec} should not be a consequence of the absence of modified nucleosides in the present tRNA transcript, as the natural tRNA^{Sec} lacks modified nucleosides in the D stem. Conversely, mcm^{5}U34 or mcm^{5}Um34, i^{6}A37, Ψ55 and m^{1}A58 exist in the vertebrate tRNA^{Sec}s (42,43). Positions 34 and 37 are in the anticodon loop, which does not participate in the tertiary interaction. The T-loop conformation involving positions 55 and 58 of tRNA^{Sec} superimposes well on those of the canonical tRNA structures with the nucleoside modifications (38,44–47); the base pairs G18:U55 and U54:A58 are formed as the canonical tertiary base pairs G18:Ψ55 and T54:m^{1}A58. Therefore, it is unlikely that the lack of these modifications either affects the D-loop:T-loop interaction or furthermore remotely alters the D stem structure.

The structure of tRNA^{Sec} had been predicted based on biochemical analyses using enzymatic and chemical probes (29,30). Structural models of both the eukaryal and bacterial tRNA^{Sec}s were reported. The study of *Xenopus laevis* tRNA^{Sec} predicted the 9/4 secondary structure of the acceptor-T stem, consistent with our crystal structure, as well as several tertiary base pairs (29). Among them, G18:U55, G19:U56 and U16:U59 were confirmed by the present structure (Figure 2B and C), but the A8:A14:U21 base triple was not present in the structure. In the crystal structure, A8 does not participate in base pairing. The U20:G19:C56 base triple and the base stacking of U9 on the G45:A48 pair were not predicted by the biochemical analyses, but they exist in the crystal structure.

Interaction with SerRS

SerRS possesses a long coiled-coil that is responsible for the tRNA binding (38). In the *T. thermophilus* SerRS•tRNA^{Ser} structure, the coiled-coil interacts with the tRNA elbow (G19:C56 pair) and the extra stem (38), and these interactions are the major determinants for the tRNA aminoacylation (49). The SerRS•tRNA^{Sec} docking model suggests that these interactions are also conserved in tRNA^{Sec} (Figure 5A and B). Since the extra-stem orientations are similar between tRNA^{Ser} and tRNA^{Sec} (Figure 4A and B), SerRS could interact with tRNA^{Sec} and tRNA^{Ser} in similar manners.

In addition to these interactions, SerRS should contact the tRNA^{Sec} acceptor arm, to ligate serine to the 3′ end. In the SerRS•tRNA^{Sec} docking model, the distance between the O3′ atom of C72 and the SerRS catalytic site is ~26 Å, which is comparable to the distance of ~24 Å in the tRNA^{Ser} complex. Although the acceptor-T stem of tRNA^{Sec} is longer than that of tRNA^{Ser}, the docking model suggests that the tRNA^{Sec} acceptor stem can place the CCA end in the SerRS catalytic site.

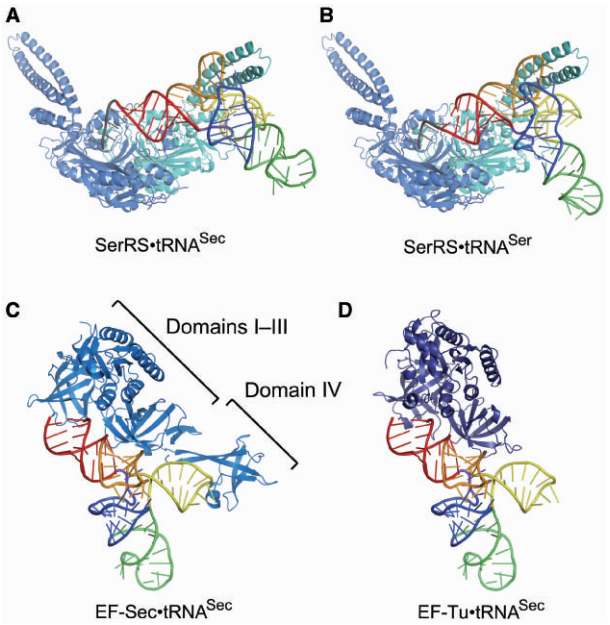

Figure 5. The docking models. (**A**) A docking model of SerRS and tRNA^{Sec}. The two subunits of the *P. horikoshii* SerRS dimer are colored sky blue and cyan, respectively. Human tRNA^{Sec} is colored as in Figure 1. (**B**) A docking model of SerRS and tRNA^{Ser}. (**C**) A docking model of EF-Sec and tRNA^{Sec}. *Methanococcus maripaludis* SelB/EF-Sec is shown as a ribbon diagram, colored marine blue. (**D**) A docking model of EF-Tu and tRNA^{Sec}. *Thermus aquaticus* EF-Tu is colored deep blue.

Interactions with PSTK and SepSecS

In eukarya, the phosphorylation of Ser-tRNA^{Sec} depends mainly on the larger number of base pairs in the D stem, rather than the long acceptor stem or extra arm (50,51). This suggests that PSTK recognizes the D stem structure as the main discrimination site. The D stem of tRNA^{Sec} is 2 bp longer than those of the canonical tRNAs, and is quite independent, lacking tertiary interactions with either the extra arm or the AD linker. These properties are responsible for the unique D-arm conformation. The D stem is shifted outward from the axis running along the anticodon stem to the T loop, resulting in a hole in place of the canonical tertiary core (Figure 4A).

In contrast, the D stem of $tRNA^{Ser}$ is tightly packed in the tertiary core. It seems reasonable that PSTK discriminates $tRNA^{Sec}$ from $tRNA^{Ser}$ by relying on the characteristic D-arm conformation of $tRNA^{Sec}$. In archaea, the second base pair of the acceptor stem is the major determinant for the $tRNA^{Sec}$ discrimination by PSTK (52). This base pair is conserved as G2:C71 and C2:G71 in $tRNA^{Sec}$ and $tRNA^{Ser}$, respectively. Conversely, in eukarya, the second base pair is conserved as C2:G71 in $tRNA^{Sec}$, but is nonconserved with some C2:G71 pairs in $tRNA^{Ser}$ (28). Therefore, the second base pair of the acceptor stem should not be important for eukaryal PSTK.

The Sec-$tRNA^{Sec}$ formation also depends on the long D stem, rather than the long extra arm (51). The length of the acceptor stem also affects the Sec-$tRNA^{Sec}$ synthesis. The reduction of the length of the acceptor stem by 1 bp decreased the Sec-$tRNA^{Sec}$ synthesis by 3–5-fold (51,53). These results suggest that SepSecS and/or PSTK recognize the unique D and acceptor stems of $tRNA^{Sec}$ as the discrimination sites. In the bacterial system, the long acceptor stem of $tRNA^{Sec}$ is important for the Sec-$tRNA^{Sec}$ synthesis by SelA (54). The long extra arm is not important, and the involvement of the D arm in the $tRNA^{Sec}$ discrimination has not been reported.

Interaction with EF-Sec

Eukaryal/archaeal EF-Sec/SelB comprises four domains: the three N-terminal domains (domains I–III) homologous to EF-Tu (or EF1A) and the unique C-terminal domain (domain IV) (41). The docking model of EF-Sec and $tRNA^{Sec}$ suggests that EF-Sec can interact with the $tRNA^{Sec}$ acceptor stem, as in the EF-Tu•$tRNA^{Phe}$ complex. The EF-Sec domain III is close to the boundary of the acceptor and T stems, and could recognize the parts characteristic of $tRNA^{Sec}$ (Figure 5C). The EF-Sec-specific domain IV is located near the $tRNA^{Sec}$ extra arm, and might also participate in the $tRNA^{Sec}$ recognition (Figure 5C). In the reported structures of EF-Tu•tRNA complexes, the tRNA acceptor-T stem is curved outward, presumably by an induced fit to EF-Tu (40,48). The bent acceptor-T stem in the present structure may mimic the EF-Sec-bound conformation of $tRNA^{Sec}$.

The docking model of EF-Tu and human $tRNA^{Sec}$ suggests that EF-Tu can interact with the $tRNA^{Sec}$ acceptor stem in a similar manner as in EF-Tu•$tRNA^{Phe}$ (Figure 5D). There are no severe steric clashes between EF-Tu and $tRNA^{Sec}$. The dissociation constant (K_d) between EF-Tu and Ser-$tRNA^{Sec}$ was reportedly 50 nM (55). The high affinity seems to be consistent with our model, although this value is about 70-fold larger than that between EF-Tu and Ser-$tRNA^{Ser}$ ($K_d = 0.7$ nM) (55). The structures of the EF-Tu•tRNA complexes suggest that the interaction depends on the conformational adaptability of the acceptor-T stem backbone to EF-Tu (40,48). The unique bending point of the human $tRNA^{Sec}$ acceptor stem might be related to the lower affinity of EF-Tu for $tRNA^{Sec}$ in comparison to $tRNA^{Ser}$.

ACCESSION NUMBER

The coordinates have been deposited in the Protein Data Bank (ID: 3A3A).

SUPPLEMENTARY DATA

Supplementary Data are available at NAR Online.

ACKNOWLEDGEMENTS

We thank the staffs of the SPring-8 BL41XU (Hyogo, Japan) and the Photon Factory beam lines (Tsukuba, Japan) for assistance with our data collection. We also thank A. Ishii and T. Nakayama for assistance in the manuscript preparation.

FUNDING

Japan Society for the Promotion of Science (JSPS) Grant-in-Aid for Scientific Research (to S.S.); JSPS Global Centers of Excellence Program (Integrative Life Science Based on the Study of Biosignaling Mechanisms); Ministry of Education, Culture, Sports, Science, and Technology Targeted Proteins Research Program; and Research Fellowships from JSPS (to Y.I.). Funding for open access charge: RIKEN

Conflict of interest statement. None declared.

REFERENCES

1. Zinoni,F., Birkmann,A., Leinfelder,W. and Böck,A. (1987) Cotranslational insertion of selenocysteine into formate dehydrogenase from *Escherichia coli* directed by a UGA codon. *Proc. Natl Acad. Sci. USA*, **84**, 3156–3160.
2. Böck,A., Forchhammer,K., Heider,J., Leinfelder,W., Sawers,G., Veprek,B. and Zinoni,F. (1991) Selenocysteine: the 21st amino acid. *Mol. Microbiol.*, **5**, 515–520.
3. Huber,R.E. and Criddle,R.S. (1967) Comparison of the chemical properties of selenocysteine and selenocystine with their sulfur analogs. *Arch. Biochem. Biophys.*, **122**, 164–173.
4. Cone,J.E., Del Rio,R.M., Davis,J.N. and Stadtman,T.C. (1976) Chemical characterization of the selenoprotein component of clostridial glycine reductase: identification of selenocysteine as the organoselenium moiety. *Proc. Natl Acad. Sci. USA*, **73**, 2659–2663.
5. Chambers,I., Frampton,J., Goldfarb,P., Affara,N., McBain,W. and Harrison,P.R. (1986) The structure of the mouse glutathione peroxidase gene: the selenocysteine in the active site is encoded by the 'termination' codon, TGA. *EMBO J.*, **5**, 1221–1227.
6. Zinoni,F., Birkmann,A., Stadtman,T.C. and Böck,A. (1986) Nucleotide sequence and expression of the selenocysteine-containing polypeptide of formate dehydrogenase (formate-hydrogen-lyase-linked) from *Escherichia coli*. *Proc. Natl Acad. Sci. USA*, **83**, 4650–4654.
7. Kryukov,G.V., Castellano,S., Novoselov,S.V., Lobanov,A.V., Zehtab,O., Guigo,R. and Gladyshev,V.N. (2003) Characterization of mammalian selenoproteomes. *Science*, **300**, 1439–1443.
8. Leinfelder,W., Zehelein,E., Mandrand-Berthelot,M.A. and Böck,A. (1988) Gene for a novel tRNA species that accepts L-serine and cotranslationally inserts selenocysteine. *Nature*, **331**, 723–725.
9. Carlson,B.A., Xu,X.M., Kryukov,G.V., Rao,M., Berry,M.J., Gladyshev,V.N. and Hatfield,D.L. (2004) Identification and characterization of phosphoseryl-$tRNA^{[Ser]Sec}$ kinase. *Proc. Natl Acad. Sci. USA*, **101**, 12848–12853.
10. Yuan,J., Palioura,S., Salazar,J.C., Su,D., O'Donoghue,P., Hohn,M.J., Cardoso,A.M., Whitman,W.B. and Söll,D. (2006) RNA-dependent conversion of phosphoserine forms selenocysteine

in eukaryotes and archaea. *Proc. Natl Acad. Sci. USA*, **103**, 18923–18927.
11. Xu,X.M., Carlson,B.A., Mix,H., Zhang,Y., Saira,K., Glass,R.S., Berry,M.J., Gladyshev,V.N. and Hatfield,D.L. (2007) Biosynthesis of selenocysteine on its tRNA in eukaryotes. *PLoS Biol.*, **5**, e4.
12. Forchhammer,K. and Böck,A. (1991) Selenocysteine synthase from *Escherichia coli*. Analysis of the reaction sequence. *J. Biol. Chem.*, **266**, 6324–6328.
13. Ehrenreich,A., Forchhammer,K., Tormay,P., Veprek,B. and Böck,A. (1992) Selenoprotein synthesis in *E. coli*. Purification and characterisation of the enzyme catalysing selenium activation. *Eur. J. Biochem.*, **206**, 767–773.
14. Low,S.C., Harney,J.W. and Berry,M.J. (1995) Cloning and functional characterization of human selenophosphate synthetase, an essential component of selenoprotein synthesis. *J. Biol. Chem.*, **270**, 21659–21664.
15. Heider,J., Baron,C. and Böck,A. (1992) Coding from a distance: dissection of the mRNA determinants required for the incorporation of selenocysteine into protein. *EMBO J.*, **11**, 3759–3766.
16. Berry,M.J., Banu,L., Harney,J.W. and Larsen,P.R. (1993) Functional characterization of the eukaryotic SECIS elements which direct selenocysteine insertion at UGA codons. *EMBO J.*, **12**, 3315–3322.
17. Forchhammer,K., Leinfelder,W. and Böck,A. (1989) Identification of a novel translation factor necessary for the incorporation of selenocysteine into protein. *Nature*, **342**, 453–456.
18. Baron,C., Heider,J. and Böck,A. (1993) Interaction of translation factor SELB with the formate dehydrogenase H selenopolypeptide mRNA. *Proc. Natl Acad. Sci. USA*, **90**, 4181–4185.
19. Yamada,K., Mizutani,T., Ejiri,S. and Totsuka,T. (1994) A factor protecting mammalian [^{75}Se]SeCys-tRNA is different from EF-1 alpha. *FEBS Lett.*, **347**, 137–142.
20. Fagegaltier,D., Hubert,N., Yamada,K., Mizutani,T., Carbon,P. and Krol,A. (2000) Characterization of mSelB, a novel mammalian elongation factor for selenoprotein translation. *EMBO J.*, **19**, 4796–4805.
21. Selmer,M. and Su,X.D. (2002) Crystal structure of an mRNA-binding fragment of *Moorella thermoacetica* elongation factor SelB. *EMBO J.*, **21**, 4145–4153.
22. Yoshizawa,S., Rasubala,L., Ose,T., Kohda,D., Fourmy,D. and Maenaka,K. (2005) Structural basis for mRNA recognition by elongation factor SelB. *Nat. Struct. Mol. Biol.*, **12**, 198–203.
23. Lesoon,A., Mehta,A., Singh,R., Chisolm,G.M. and Driscoll,D.M. (1997) An RNA-binding protein recognizes a mammalian selenocysteine insertion sequence element required for cotranslational incorporation of selenocysteine. *Mol. Cell Biol.*, **17**, 1977–1985.
24. Rother,M., Wilting,R., Commans,S. and Böck,A. (2000) Identification and characterisation of the selenocysteine-specific translation factor SelB from the archaeon *Methanococcus jannaschii*. *J. Mol. Biol.*, **299**, 351–358.
25. Copeland,P.R., Fletcher,J.E., Carlson,B.A., Hatfield,D.L. and Driscoll,D.M. (2000) A novel RNA binding protein, SBP2, is required for the translation of mammalian selenoprotein mRNAs. *EMBO J.*, **19**, 306–314.
26. Ding,F. and Grabowski,P.J. (1999) Identification of a protein component of a mammalian tRNA^{Sec} complex implicated in the decoding of UGA as selenocysteine. *RNA*, **5**, 1561–1569.
27. Xu,X.M., Mix,H., Carlson,B.A., Grabowski,P.J., Gladyshev,V.N., Berry,M.J. and Hatfield,D.L. (2005) Evidence for direct roles of two additional factors, SECp43 and soluble liver antigen, in the selenoprotein synthesis machinery. *J. Biol. Chem.*, **280**, 41568–41575.
28. Jühling,F., Mörl,M., Hartmann,R.K., Sprinzl,M., Stadler,P.F. and Pütz,J. (2009) tRNAdb 2009: compilation of tRNA sequences and tRNA genes. *Nucleic Acids Res.*, **37**, D159–D162.
29. Sturchler,C., Westhof,E., Carbon,P. and Krol,A. (1993) Unique secondary and tertiary structural features of the eucaryotic selenocysteine tRNA^{Sec}. *Nucleic Acids Res.*, **21**, 1073–1079.
30. Baron,C., Westhof,E., Böck,A. and Giegé,R. (1993) Solution structure of selenocysteine-inserting tRNA^{Sec} from *Escherichia coli*. Comparison with canonical tRNA^{Ser}. *J. Mol. Biol.*, **231**, 274–292.
31. Sekine,S., Nureki,O., Sakamoto,K., Niimi,T., Tateno,M., Go,M., Kohno,T., Brisson,A., Lapointe,J. and Yokoyama,S. (1996) Major identity determinants in the "augmented D helix" of tRNA^{Glu} from *Escherichia coli*. *J. Mol. Biol.*, **256**, 685–700.
32. Otwinowski,Z. and Minor,W. (1997) Processing of X-ray diffraction data collected in oscillation mode. *Methods Enzymol.*, **276**, 307–326.
33. Read,R.J. (2001) Pushing the boundaries of molecular replacement with maximum likelihood. *Acta Crystallogr. D*, **57**, 1373–1382.
34. Westhof,E., Dumas,P. and Moras,D. (1988) Restrained refinement of two crystalline forms of yeast aspartic acid and phenylalanine transfer RNA crystals. *Acta Crystallogr. A*, **44** (Pt 2), 112–123.
35. Sussman,J.L., Holbrook,S.R., Warrant,R.W., Church,G.M. and Kim,S.H. (1978) Crystal structure of yeast phenylalanine transfer RNA. I. Crystallographic refinement. *J. Mol. Biol.*, **123**, 607–630.
36. Adams,P.D., Pannu,N.S., Read,R.J. and Brunger,A.T. (1997) Cross-validated maximum likelihood enhances crystallographic simulated annealing refinement. *Proc. Natl Acad. Sci. USA*, **94**, 5018–5023.
37. Emsley,P. and Cowtan,K. (2004) Coot: model-building tools for molecular graphics. *Acta Crystallogr. D Biol. Crystallogr.*, **60**, 2126–2132.
38. Biou,V., Yaremchuk,A., Tukalo,M. and Cusack,S. (1994) The 2.9 Å crystal structure of *T. thermophilus* seryl-tRNA synthetase complexed with tRNA^{Ser}. *Science*, **263**, 1404–1410.
39. Itoh,Y., Sekine,S., Kuroishi,C., Terada,T., Shirouzu,M., Kuramitsu,S. and Yokoyama,S. (2008) Crystallographic and mutational studies of seryl-tRNA synthetase from the archaeon *Pyrococcus horikoshii*. *RNA Biol.*, **5**, 169–177.
40. Nissen,P., Kjeldgaard,M., Thirup,S., Polekhina,G., Reshetnikova,L., Clark,B.F. and Nyborg,J. (1995) Crystal structure of the ternary complex of Phe-tRNA^{Phe}, EF-Tu, and a GTP analog. *Science*, **270**, 1464–1472.
41. Leibundgut,M., Frick,C., Thanbichler,M., Böck,A. and Ban,N. (2005) Selenocysteine tRNA-specific elongation factor SelB is a structural chimaera of elongation and initiation factors. *EMBO J.*, **24**, 11–22.
42. Diamond,A.M., Choi,I.S., Crain,P.F., Hashizume,T., Pomerantz,S.C., Cruz,R., Steer,C.J., Hill,K.E., Burk,R.F., McCloskey,J.A. *et al.* (1993) Dietary selenium affects methylation of the wobble nucleoside in the anticodon of selenocysteine tRNA$^{[Ser]Sec}$. *J. Biol. Chem.*, **268**, 14215–14223.
43. Sturchler,C., Lescure,A., Keith,G., Carbon,P. and Krol,A. (1994) Base modification pattern at the wobble position of *Xenopus* selenocysteine tRNA^{Sec}. *Nucleic Acids Res.*, **22**, 1354–1358.
44. Robertus,J.D., Ladner,J.E., Finch,J.T., Rhodes,D., Brown,R.S., Clark,B.F. and Klug,A. (1974) Structure of yeast phenylalanine tRNA at 3 Å resolution. *Nature*, **250**, 546–551.
45. Kim,S.H., Suddath,F.L., Quigley,G.J., McPherson,A., Sussman,J.L., Wang,A.H., Seeman,N.C. and Rich,A. (1974) Three-dimensional tertiary structure of yeast phenylalanine transfer RNA. *Science*, **185**, 435–440.
46. Moras,D., Comarmond,M.B., Fischer,J., Weiss,R., Thierry,J.C., Ebel,J.P. and Giegé,R. (1980) Crystal structure of yeast tRNA^{Asp}. *Nature*, **288**, 669–674.
47. Hingerty,B., Brown,R.S. and Jack,A. (1978) Further refinement of the structure of yeast tRNA^{Phe}. *J. Mol. Biol.*, **124**, 523–534.
48. Nissen,P., Thirup,S., Kjeldgaard,M. and Nyborg,J. (1999) The crystal structure of Cys-tRNA^{Cys}-EF-Tu-GDPNP reveals general and specific features in the ternary complex and in tRNA. *Structure*, **7**, 143–156.
49. Wu,X.Q. and Gross,H.J. (1993) The long extra arms of human tRNA$^{(Ser)Sec}$ and tRNA^{Ser} function as major identify elements for serylation in an orientation-dependent, but not sequence-specific manner. *Nucleic Acids Res.*, **21**, 5589–5594.
50. Wu,X.Q. and Gross,H.J. (1994) The length and the secondary structure of the D-stem of human selenocysteine tRNA are the major identity determinants for serine phosphorylation. *EMBO J.*, **13**, 241–248.
51. Amberg,R., Mizutani,T., Wu,X.Q. and Gross,H.J. (1996) Selenocysteine synthesis in mammalia: an identity switch from tRNA^{Ser} to tRNA^{Sec}. *J. Mol. Biol.*, **263**, 8–19.
52. Sherrer,R.L., Ho,J.M. and Söll,D. (2008) Divergence of selenocysteine tRNA recognition by archaeal and eukaryotic *O*-phosphoseryl-tRNA^{Sec} kinase. *Nucleic Acids Res.*, **36**, 1871–1880.

53. Sturchler-Pierrat,C., Hubert,N., Totsuka,T., Mizutani,T., Carbon,P. and Krol,A. (1995) Selenocysteylation in eukaryotes necessitates the uniquely long aminoacyl acceptor stem of selenocysteine $tRNA^{Sec}$. *J. Biol. Chem.*, **270**, 18570–18574.
54. Baron,C. and Böck,A. (1991) The length of the aminoacyl-acceptor stem of the selenocysteine-specific $tRNA^{Sec}$ of *Escherichia coli* is the determinant for binding to elongation factors SELB or Tu. *J. Biol. Chem.*, **266**, 20375–20379.
55. Förster,C., Ott,G., Forchhammer,K. and Sprinzl,M. (1990) Interaction of a selenocysteine-incorporating tRNA with elongation factor Tu from *E.coli*. *Nucleic Acids Res.*, **18**, 487–491.